J. Membrane Biol. 143, 153–163 (1995)

The Journal of
Membrane
Biology

Voltage-dependent Sodium Channels in Human Small-Cell Lung Cancer Cells: Role in Action Potentials and Inhibition by Lambert-Eaton Syndrome IgG

J.K.W. Blandino[1], M.P. Viglione[2], W.A. Bradley[1], H.K. Oie[3], Y.I. Kim[1,4]

[1]Department of Biomedical Engineering, University of Virginia School of Medicine, Box 377, Charlottesville, Virginia 22908
[2]Department of Neuroscience, University of Virginia School of Medicine, Charlottesville, Virginia 22908
[3]National Cancer Institute, Navy Medical Oncology Branch, Naval Hospital, Bethesda, Maryland 20892
[4]Department of Neurology, University of Virginia School of Medicine, Charlottesville, Virginia 22908

Received: 18 July 1994/Revised: 14 October 1994

Abstract. Sodium channels of human small-cell lung cancer (SCLC) cells were examined with whole-cell and single-channel patch clamp methods. In the tumor cells from SCLC cell line NCI-H146, the majority of the voltage-gated Na^+ channels are only weakly tetrodotoxin (TTX)-sensitive (K_d = 215 nM). With the membrane potential maintained at −60 to −80 mV, these cells produced all-or-nothing action potentials in response to depolarizing current injection (>20 pA). Similar all-or-nothing spikes were also observed with anodal break excitation. Removal of external Ca^{2+} did not affect the action potential production, whereas 5 μM TTX or substitution of Na^+ with choline abolished it. Action potentials elicited in the Ca^{2+}-free condition were reversibly blocked by 4 mM $MnCl_2$ due to the Mn^{2+}-induced inhibition of voltage-dependent sodium currents (I_{Na}). Therefore, Na^+ channels, not Ca^{2+} channels, underlie the excitability of SCLC cells. Whole-cell I_{Na} was maximal with step-depolarizing stimulations to 0 mV, and reversed at +45.2 mV, in accord with the predicted Nernst equilibrium potential for a Na^+-selective channel. I_{Na} evoked by depolarizing test potentials (−60 to +40 mV) exhibited a transient time course and activation/inactivation kinetics typical of neuronal excitable membranes; the plot of the Hodgkin-Huxley parameters, m_∞ and h_∞, also revealed biophysical similarity between SCLC and neuronal Na^+ channels. The single channel current amplitude, as measured with the inside-out patch configuration, was 1.0 pA at −20 mV with a slope conductance of 12.1 pS. The autoantibodies implicated in the Lambert-Eaton myasthenic syndrome (LES), which are known to inhibit I_{Ca} and I_{Na} in bovine adrenal chromaffin cells, also significantly inhibited I_{Na} in SCLC cells. These results indicate that (i) action potentials in human SCLC cells result from the regenerative increase in voltage-gated Na^+ channel conductance; (ii) fundamental characteristics of SCLC Na^+ channels are the same as the classical sodium channels found in a variety of excitable cells; and (iii) in some LES patients, SCLC Na^+ channels are an additional target of the pathological IgG present in the patients' sera.

Key words: Small-cell lung cancer cells — Voltage-gated sodium channels — Action potentials — Lambert-Eaton syndrome — Paraneoplastic neurological disorders

Introduction

Small-cell lung cancer is a highly malignant tumor that accounts for about 25% of lung cancers (Carney, 1992). A remarkable feature of SCLC is that it is the most commonly encountered form of neoplasm associated with a wide range of paraneoplastic neurological disorders (Anderson, Cunningham & Posner, 1987). Although the etiology whereby SCLC produces "remote effects" on the nervous system is not precisely known, evidence for autoimmunity is compelling in some paraneoplastic disorders. One of the most well-studied SCLC-associated neurological disorders is the Lambert-Eaton myasthenic syndrome (*reviewed in* Vincent, Lang & Newsom-Davis, 1989), a neuromuscular disease characterized by the insufficient release of acetylcholine from the motor nerve terminal (Elmqvist & Lambert, 1968). It is now well established that the pathological

Correspondence to: Y.I. Kim, Department of Biomedical Engineering

Table. Composition of internal and external solutions for patch clamp recordings

	External solution (mM)				Internal solution (mM)		
	I	II	III	IV	V	VI	VII
NaCl	140	140		70		5	
KCl	2.8	2.8	2.8	2.8		129	129
$CaCl_2$	2		2		1	1	1
$MgCl_2$	2	2	2	2	2	2	2
Choline Chloride			150	70			
$CsCl_2$					120		
$CoCl_2$		1		1			
TEA-Cl					20		
NaOH-EGTA					11		
NaOH-HEPES	10	10		10	10		
KOH-EGTA						11	11
KOH-HEPES						10	10
HEPES			10				
pH adj. to 7.2 with:	NaOH	NaOH	KOH	NaOH	TEA-OH	KOH	KOH

autoantibodies in LES cause the dysfunction of voltage-gated Ca^{2+} channels (Roberts et al., 1985; Kim & Neher, 1988; Peers et al., 1990). These findings thus lead to the supposition that Ca^{2+} channels in SCLC cells serve as the antigenic source for the production of the antibodies. In addition, as demonstrated in lymphocytes (Decoursey et al., 1984) and tumors of the nervous system (Lee, Weber & Wurster, 1992), K^+ and Ca^{2+} channels in SCLC cells may also play a role in cell proliferation (Pancrazio et al., 1991). In view of the involvement of SCLC ion channels as antigens in the paraneoplastic disease process, patch clamp characterization of these ion channels would increase understanding of their antigenic features.

The purpose of the present study is twofold. First, it is aimed at characterizing the voltage-dependent Na^+ channels in these tumor cells using electrophysiological criteria and determining the putative role of Na^+ and Ca^{2+} currents in the production of action potentials. Until recently, there has been a paucity of information on the voltage-gated ion channels expressed by human SCLC cells. Although recent patch clamp studies have identified the existence of Na^+, K^+, and Ca^{2+} channels in SCLC cell lines (Johansson et al., 1989; Pancrazio et al., 1989; Pancrazio et al., 1991; Pancrazio, Oie & Kim, 1992), a detailed biophysical and pharmacological characterization of these ion channels has yet to be established. Earlier studies (Tischler, Dichter & Biales, 1977) demonstrated that SCLC cells are neuroendocrine-like cells capable of producing action potentials. It has also been reported that action potentials in these tumor cells are caused by Ca^{2+} and Ca^{2+}-activated potassium currents (McCann et al., 1981). However, the patch clamp finding that SCLC cells possess voltage-dependent Na^+ channels (Johansson et al., 1989; Pancrazio et al., 1989) suggests the possible role of Na^+ channels in action potential production and propagation, a function revealed in a variety of classical excitable membranes.

The second objective was to examine the possibility that LES antibodies cross-react with Na^+ channels in SCLC cells. Although the antibody-induced inhibition of the presynaptic Ca^{2+} channels is clearly the primary pathogenic mechanism underlying LES, a previous study of I_{Na} in bovine adrenal chromaffin cells (Viglione, Creutz & Kim, 1992) revealed that in about 30% of patients with LES, the pathological antibodies also reduced I_{Na}. In LES associated with cancer, SCLC cells are likely to be the source of antigenic stimulation. Thus, it is important to determine whether I_{Na} in SCLC cells is similarly reduced by LES IgG and to ascertain the reactivity of the LES antibodies with Na^+ channels.

Materials and Methods

Cell Culture

The human SCLC cell line NCI-H146 was established at the Navy Medical Oncology Branch of the National Cancer Institute (Bethesda, MD) and transferred to the University of Virginia. Cells were maintained in RPMI 1640 media with 10% heat-inactivated fetal bovine serum (GIBCO, Grand Island, NY). Flasks containing cells were incubated at 37°C in 5% CO_2 and 95% air. Cells were subcultured by mechanical dissociation once per week. For each experiment, cells were triturated and then affixed to glass coverslips coated with poly-L-lysine (Sigma Chemical, St. Louis, MO).

Solutions

The Table lists the composition of solutions used in the pipette and external bath for all patch clamp experiments and action potential measurements. Specific solutions used in different types of measurements are indicated in the text and figure legends. For the experiments involving delivery or washout of drugs into the patch clamp recording chamber, a gravity perfusion system was used.

Current-Clamp Experiments

Data on transmembrane voltage and action potentials were obtained from current-clamped SCLC cells that were subject to the whole-cell recording configuration (Hamill et al., 1981) using a List EPC-7 patch clamp amplifier (List Electronic, Darmstadt, Germany). The resting membrane potential was determined 40 sec after achieving the whole-cell configuration to ensure the stability by allowing maximum diffusion of the pipette solution into the cell. Steady transmembrane current, generated by a Grass S-88 stimulator (Grass Instruments, Quincy, MA), was injected to hold the cell at about −80 mV. The cells were then stimulated with current pulses of 20 msec in duration at a rate of 0.5 Hz, the amplitude of which ranged from 20 to 80 pA, sufficient to depolarize the cell membrane just above the action potential threshold. The duration of the action potential was measured from the rising phase at threshold to the falling phase that crossed the threshold. In calculating the maximum derivative of the action potential, the forward difference method was applied to the digitized signal, while the current measured at 20 mV depolarization from holding potential of −80 mV was used to calculate the input resistance R_i of the cell.

Studies of TTX Sensitivity

A 0.25 mg/ml stock solution of tetrodotoxin (Sigma) was made in distilled water, stored at 4°C before use, and added to the bath to achieve the desired final concentration. In an attempt to determine the half-maximal blockade of I_{Na} by TTX, we fit the data with a one-to-one receptor binding model (Antoni, Böcker & Eickhorn, 1988):

$$I_{Na}/I_{Na,max} = 1/(1 + [TTX]/K_d) \quad (1)$$

where K_d is the dissociation constant of the TTX-receptor complex and [TTX] is the concentration of TTX. The result was then compared with a fit to the noncooperative, two-site model (Weiss & Sidell, 1991):

$$I_{Na[TTX]}/I_{Na} = K_S(1 - I_R/I_{Na})/(K_S + [TTX]) + K_R(I_R/I_{Na})/(K_R + [TTX]) \quad (2)$$

where $I_{Na[TTX]}$ and I_{Na} are, respectively, the sodium current measured in the presence and absence of TTX. I_R is the maximum TTX-resistant sodium current. K_S and K_R are the equilibrium dissociation constants for TTX-sensitive and TTX-resistant channels, respectively.

Whole-Cell I_{Na} and Single Na^+ Channel Currents

Whole-cell and inside-out single-channel patch clamp recording configurations were used according to the method of Hamill et al. (1981). All experiments were conducted at room temperature (23 to 25°C). The data acquisition and analysis method was the same as Pancrazio et al. (1989). Briefly, I_{Na} was recorded one minute after establishing the whole-cell configuration using a List EPC-7 patch clamp amplifier. The cells were stimulated with voltage pulses of 40 msec duration at a rate of 0.5 Hz from the holding potential of −80 mV. The Na^+ activation parameters were studied using the pCLAMP software on an IBM PC compatible 386 computer equipped with a Labmaster DMA data acquisition system (Scientific Solutions, Solon, OH). Data were sampled at 50 kHz and analyzed later. Leakage subtraction was done online using a P/4 protocol.

All single channel recordings were carried out using the inside-out membrane patches and analyzed by the pCLAMP software. Current records of 90 msec duration were obtained with the depolarizing command potentials at a rate of 0.5 Hz from a V_h of −80 mV. The recorded data were multiplied by a digitized Gaussian filter with 1 kHz cutoff frequency before the analysis.

Incubation of SCLC Cells with LES Serum and IgG

The use of human plasma and the procedures for obtaining serum and isolating IgG have been described previously (Kim & Neher, 1988; Vigilione et al., 1992). Plasma and sera were obtained from three patients who were clinically and electromyographically diagnosed as having LES. The disorders of Patients 1 and 2 were associated with SCLC, while Patient 3 had no evidence of malignancy.

Statistics

Where appropriate, results are presented as the mean ± SEM and the number of cells tested. To compare currents between different groups, currents were normalized by the cell capacitance first to eliminate the variability of cell size. The significant difference between groups was determined using Student's t-test. A P value of <0.05 was considered significant.

Results

Transmembrane Voltage and Action Potentials in H146 Cells

When physiological concentrations of Na^+, K^+, and Ca^{2+} ions were used in both the extracellular and intracellular solutions (*see* the Table, solutions I and VI), the resting membrane potential of the SCLC H146 cells was −43.7 ± 1.5 mV (n = 14 cells, C_m = 7.3 ± 1.3 pF) with an input resistance of 5.9 ± 1.7 GΩ (n = 12). The membrane potential was found to be more negative than that reported by Johansson et al. (1989) and McCann et al. (1981) for the cell lines U1690 (−29 mV) and DMS 53 (−32.8 mV), respectively.

Figure 1*A* displays the representative changes in transmembrane potential occurring at different levels of current injection for an H146 cell. Injection of subthreshold current (<25 pA) produced a graded response characteristic of the electronic potential. With suprathreshold current, all-or-nothing action potentials were elicited, which rose from the clamped potential of −78.8 ± 2.4 mV and rapidly surpassed 0 mV, peaking at 19.2 ± 4.6 mV; dV/dt_{max} was 41.0 ± 7.8 V/sec. The estimated threshold for generating the action potentials was −35.2 ± 2.8 mV (n = 14). Of 29 H146 cells injected with suprathreshold depolarizing current, all-or-nothing-type spiking could be observed in 27 cells; the remaining 2 cells exhibited spontaneous action potentials. In all cells tested, we found no evidence that the repolarizing phase of the spikes had a discernible plateau, a characteristic of calcium spikes frequently observed in cardiac ventricular cells (Isenberg & Klöckner, 1982).

Role of Na^+ and Ca^{2+} Currents in Action Potential Generation

The work of McCann et al. (1981) concludes that the action potentials of DMS 53 SCLC cells are attributable

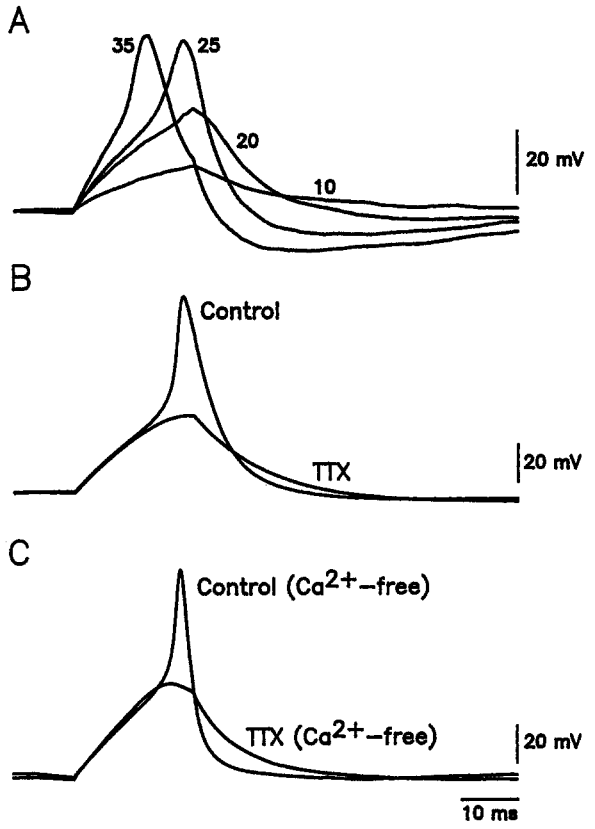

Fig. 1. Transmembrane voltage responses of NCI-H146 cells in normal and Ca^{2+}-free bath. (*A*) Voltage records produced by the injection of depolarizing currents, 10, 20, 25, and 35 pA, 20 msec in duration. The membrane potential was clamped to –74 mV. Current was injected at a rate of 0.5 Hz. Currents greater than 20 pA triggered an action potential. Solution I (*see* Table) was used in the bath and solution VI was used inside the pipette. (*B*) The action potential before (*Control*) and after (*TTX*) the addition of 5 μM TTX. Membrane potential was maintained at –66 mV before the action potential. (*C*) In Ca^{2+}-free bath containing 1 mM $CoCl_2$ (solution II), a depolarizing current elicited an action potential (*Control*) which is abolished by 5 μM TTX (*TTX*). Clamped membrane potential was –72 mV.

to the activation of voltage-gated Ca^{2+} channels and Ca^{2+}-activated K^+ channels. However, a more recent study of another SCLC cell line, U1690, does not support this notion (Johansson et al., 1989). In view of these conflicting observations, we examined the identity of currents and ions responsible for the generation of action potentials in H146 cells.

When added to the bath, TTX (5 or 15 μM) completely abolished action potentials ($n = 15$), regardless of the presence of extracellular Ca^{2+} ions (Fig. 1*B* and *C*). Replacing Na^+ with choline in the bath (solution III) similarly inhibited action potentials ($n = 3$). Conversely, action potentials persisted in cells exposed to bath solution without Ca^{2+} and with 1 mM $CoCl_2$ (Fig. 1*C*). Under this condition, spikes elicited had a threshold of -36.3 ± 1.8 mV, with a peak appearing at 15.4 ± 3.5 mV, and dV/dt_{max} of 34.5 ± 4.9 V/sec ($n = 13$). These values were not significantly different from those measured using physiological solutions as described above. It is also noteworthy that the stimulated response observed after TTX or 0 Na^+ treatment did not demonstrate any recognizable spike component other than the passive electrotonic potentials.

Prior to the measurements of the action potentials, we also recorded the macroscopic whole-cell currents from each cell. In all cells that had evoked action potentials, a large transient inward current (I_{Na}) followed by a large outward current (mostly potassium current, I_K) was consistently conserved (*see* Fig. 3*A*). Removal of extracellular Ca^{2+} ions had negligible effect on these currents, further supporting the notion that the primarily ionic carriers in the excited SCLC cell membrane are Na^+ and K^+.

These findings led us to conclude that the voltage-dependent activation of I_{Na}, along with the presumed delayed activation of I_K, is sufficient to produce transmembrane action potentials in SCLC H146 cells and that extracellular Ca^{2+} ions are not essential.

Effects of $MnCl_2$ on I_{Na}, I_{Ca} and Action Potentials in SCLC Cells

Mn^{2+} has been used as a specific blocker of Ca^{2+} channels in SCLC cells (McCann et al., 1981); however, Mn^{2+} is also known to affect Na^+ channel conductance in myelinated fibers of *Xenopus laevis* (Åhrem, 1980). Therefore, we first assessed the possible inhibitory effect of Mn^{2+} on I_{Na} of H146 cells. Both I_{Na} and I_{Ca} were measured in response to a depolarization to –10 mV from a V_h of –80 mV (Fig. 2*A*). The bath was then perfused with solution containing 4 mM $MnCl_2$. Results from four cells showed that 4 mM $MnCl_2$ reduced I_{Na} by $30.9 \pm 8.0\%$ and I_{Ca} by $76.8 \pm 5.2\%$. Thus, Mn^{2+} not only inhibited I_{Ca} but also significantly compromised the I_{Na} of SCLC cells.

Based on these findings, we surmised that the $MnCl_2$-induced failure in action potential generation could be the consequence of reduced I_{Na}, rather than I_{Ca}. To test this possibility, we exposed H146 cells to Ca^{2+}-free solution and examined the blocking action of 4 mM $MnCl_2$ on action potentials. In these experiments, we used anodal break excitation to produce the spike, the same method used by McCann et al. (1981). As illustrated in Fig. 2*B*, action potentials could be evoked in a Ca^{2+}-free bath (solution II) at the end of the hyperpolarizing stimulating current pulse. Shortly after the cell was perfused with Ca^{2+}-free solution containing 4 mM $MnCl_2$, action potentials were no longer observed. Spikes reappeared when the cell was washed with the Ca^{2+}-free solution devoid of $MnCl_2$.

These results clearly indicate that Ca^{2+} channels are not required for the action potential generation; rather, as

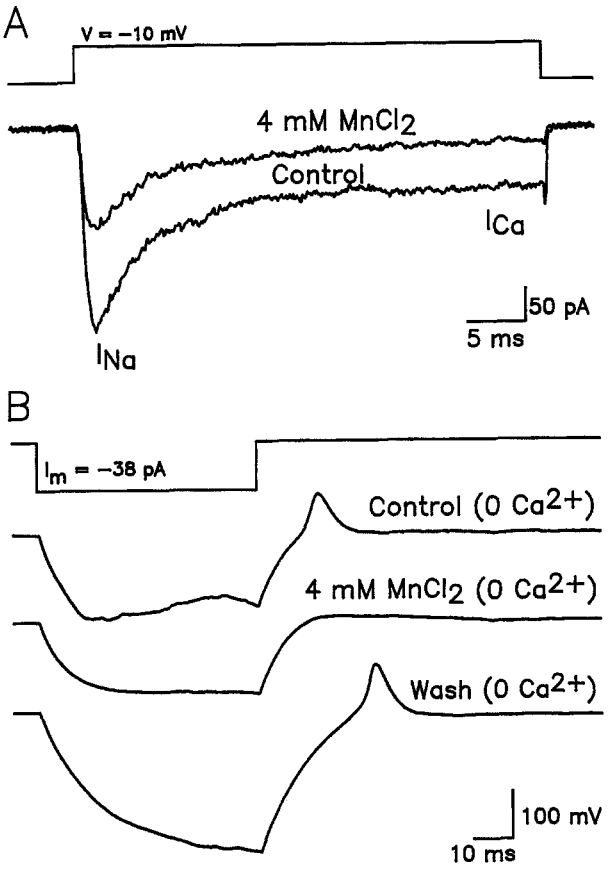

Fig. 2. Effects of 4 mM $MnCl_2$ on I_{Na}, I_{Ca} and the action potentials produced by anodal break excitation in H146 cells. (*A*) Whole-cell membrane currents of 40 msec duration occurring in response to a −10 mV depolarizing test potential from a V_h of −80 mV. I_{Na} and I_{Ca} were measured before (*Control*) and after the cell was exposed to 4 mM $MnCl_2$ for 1 min and 20 sec. Solutions I and V were used in the bath and inside the pipette, respectively. (*B*) From a different cell perfused with Ca^{2+}-free external solution, a hyperpolarizing current of 38 pA was given for 56 msec duration to generate an action potential (first trace). Solution II was used for the bath and the pipette contained solution VII. While continuously perfusing the cell with the same Ca^{2+}-free solution, 4 mM $MnCl_2$ was applied to the bath. The action potential disappeared within 4 min after the $MnCl_2$ treatment (second trace). Four minutes after washing the bath with control Ca^{2+}-free solution, the action potential response to anodal break currents was restored (third trace).

in many other neuronal and endocrine excitable membranes, the regenerative increase in Na^+ channel conductance is a key event underlying the spiking behavior of SCLC cells.

Properties of Voltage-dependent Sodium Current in H146 Cells

In view of the essential role of Na^+ channels in the tumor-cell action potential generation, we further characterized the biophysical and pharmacological behavior of the Na^+ channels in SCLC cells and compared the results with those demonstrated in typical excitable membranes.

Whole-cell I_{Na}

Figure 3 illustrates a family of whole-cell currents of voltage-clamped SCLC cells occurring in response to step depolarizations ranging from −40 to +90 mV (V_h = −80 mV). As in typical neuronal and muscle cells, a rapid inward current was followed by a delayed outward current which appeared at more positive depolarizing potentials (>−20 mV) (Fig. 3*A*). The outward currents disappeared when CsCl and tetraethylammonium (TEA) were applied internally, indicating that they are mainly carried by K^+ ions (Fig. 3*B*). The inward currents thus obtained consistently exhibited two components clearly distinguishable by different inactivation phases; a rapid transient component preceded a steady-state component with little inactivation. The size of the noninactivating current increased with elevated extracellular calcium concentration ($[Ca^{2+}]_o$), while the current could be totally eliminated with the exposure to either Ca^{2+}-free or $CoCl_2$-containing solution. This indicated that this steady-state current was carried by Ca^{2+} ions.

The notion of Na^+ as the ionic carrier of the remaining inward current (Fig. 3*C*), measured in the presence of Cs^+, TEA and under Ca^{2+}-free conditions, was supported by the following: (i) time elapsed for complete activation and inactivation of the current was less than 15 msec; (ii) the current exhibited strong voltage dependence with its peak around 0 mV; (iii) reversal potential for this current, V_{Na}, closely coincided with the Nernst equilibrium potential for Na^+; (iv) 5 μM TTX completely blocked this current; (v) when Na^+ was partially replaced by choline, the size of the resulting current was reduced with the corresponding negative shift of V_{Na}; and (vi) as explained earlier, all-or-nothing action potentials fail to occur in the absence of this current.

The macroscopic whole-cell I_{Na} exhibited a transient time course in which the currents rapidly increased to peak (1.7 ± 0.2 msec at 0 mV) and then declined exponentially to the baseline within 15 msec. Such temporal behavior is characteristic of sodium currents in neurons (Carbone & Lux, 1986; Barres, Chun & Corey, 1989), endocrine cells (Fenwick, Marty & Neher, 1982; Plant, 1988), and muscle fibers (Antoni et al., 1988).

Shown in Fig. 4*A* are a family of the rapidly activating inward currents at different depolarizations of an H146 cell. The corresponding current to voltage (*I-V*) relationship appears in Fig. 4*B*. At a V_h of −80 mV, I_{Na} was elicited from test potentials of −60 to +60 mV. The peak I_{Na} in 18 H146 cells averaged 482.5 ± 74.4 pA (n = 18, C_m = 6.8 ± 0.5 pF) and occurred between −10 and 10 mV. The reversal potential for Na^+ was 45.2 ± 1.5 mV (n = 18). Given the intracellular and extracellular

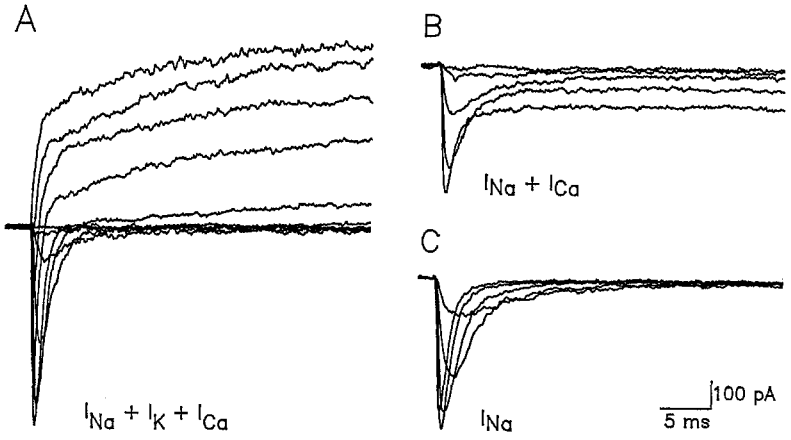

Fig. 3. Macroscopic whole-cell currents in voltage-clamped H146 cells. V_h for all cells were −80 mV. (*A*) Inward and outward current traces evoked with depolarizing test potentials from −40 to +90 with 10 mV increments, in the presence of high K^+ in the pipette (solution VII) and solution I in the bath. (*B*) When internal K^+ ions were replaced with CsCl and TEA-Cl (solution V), the outward currents were eliminated. The bath solution contained 10 mM Ca^{2+}. Test potentials were −30 to +10 mV. (*C*) Removal of external Ca^{2+} ions (solution II) resulted in abolishment of the steady-state current component, leaving only the transient Na^+ currents. Test potentials were −40 to +10 mV.

Na^+ ion concentrations of 26.9 and 142.7 mM, respectively, this value is close to that predicted by the Nernst equation (42.2 mV). This indicates a high degree of ion selectivity for H146 Na^+ channels. Reducing the extracellular Na^+ ion concentration to 72.7 mM decreased the peak I_{Na} to 110.3 ± 25.8 pA (n = 9) and shifted the *I-V* curve to the left such that the peak I_{Na} occurred between −30 and 0 mV (Fig. 4*B*). Likewise, the V_{Na} was shifted to 17.1 ± 1.4 mV (n = 9), which deviated somewhat from the estimated Nernst equilibrium potential, 25.1 mV.

Sensitivity of I_{Na} to TTX

Our next experiments were aimed at determining whether Na^+ channels in SCLC cells are of the TTX-sensitive or TTX-resistant type. Externally applied TTX suppressed I_{Na} in a dose-dependent manner (Fig. 5), with a complete blockade observed at 5 μM. Figure 4 displays a family of Na^+ current traces and the corresponding *I-V* curve from an H146 cell before and after the application of 100 nM TTX. Data were fit with Eqs. (1) and (2). The least square error criteria determined that the optimum fit was found with Eq. (1), representing the one-to-one receptor binding scheme. The calculated K_d based on Eq. (1) was 215 nM, one to two orders of magnitude higher than the values found for TTX-sensitive Na^+ channels (Weiss & Horn, 1986; Weiss & Sidell, 1991; Ogata & Tatebayashi, 1992). This K_d suggests that SCLC Na^+ channels are only modestly sensitive to TTX and may be classified as "TTX-resistant" (Weiss & Sidell, 1991; Ogata & Tatebayashi, 1992).

Activation and Inactivation Kinetics of I_{Na}

Similar to Na^+ channels in neuronal preparations, g_{Na} increased with increasing depolarization, and reached a maximum at 0 mV. In contrast, the time to peak, t_p, decreases with increasing depolarization, declining from 2.3 to 0.7 msec between −30 and +30 mV. The rising phase of I_{Na} was best described with the third power of an exponential equation (*see* Fig. 6). Figure 6*A* depicts that τ_m decreased from 0.3 to 0.08 msec between −30 and +40 mV of depolarization. Likewise, I_{Na} inactivated with a single exponential time constant, τ_h, of 11.9 msec at −30 mV and progressively declined to 0.8 msec at +30 mV of depolarization (Fig. 6*A*).

The Hodgkin-Huxley steady-state activation parameter m_∞ (Hodgkin & Huxley, 1952) and inactivation parameter, h_∞, were constructed in Fig. 6*B*. The half-activated potential, $V_{1/2}$, ranged from −23.0 to −38.8 mV with an average of −30.1 ± 1.1 mV (n = 15) and a_m varied from 10 to 20 mV with an average of 14.0 ± 1.0 mV. The steady-state inactivation curve estimated the average $V_{1/2}$ and a_h from six cells to be −42.8 ± 2.1 and 7.4 ± 0.9 mV, respectively.

Characteristics of Single Na^+ Channels

Using a pipette solution free of Ca^{2+} and an external solution containing Cs^+ and TEA, single Na^+ channel currents were studied in the inside-out membrane patch configuration. At −80 mV, no channel openings were observed during the 90 msec sampling period. Occasional openings for test pulses greater than −80 and less than −50 mV could be recorded with openings becoming more frequent with more positive depolarizations. As shown in Fig. 7*A*, the opening of Na^+ channels occurred shortly after the onset of depolarizations and subsequently disappeared. Addition of 5 μM TTX to the bath completely inhibited the openings of these channels. The amplitude, open time and closed time of the single channel events were computed from the idealized records. The amplitude histogram of unitary Na^+ currents was characterized by a Gaussian distribution (Fig. 7*B*), with its mean amplitude at −20 mV of 1.0 ± 0.06 pA (n = 4). Analysis of the single channel currents measured between −30 and 0 mV yielded the average slope conductance, 12.1 ± 3.3 pS (n = 4). The open time histogram (Fig. 7*C*) was best described by a single exponential function. At a depolarization of −20 mV, the average channel open time was 0.6 ± 0.1 msec (n = 4).

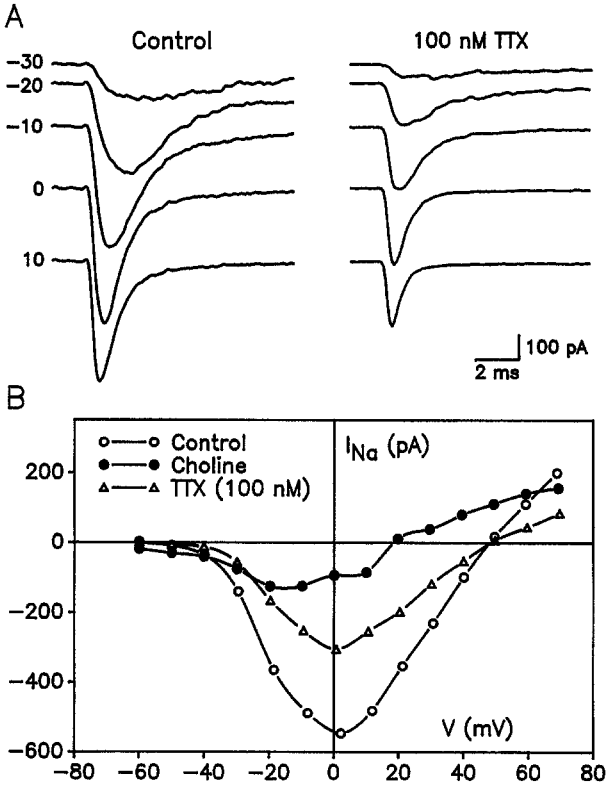

Fig. 4. Voltage-dependent sodium currents (I_{Na}) recorded from H146 cells. (*A*) Whole-cell currents were evoked from depolarizing test potentials of 40 msec duration, varying from −30 to +10 mV with 10 mV increments (*Control*). V_h was −80 mV. The pipette was filled with solution V and the bath had solution II. The right panel illustrates Na^+ current traces obtained from a cell treated with 100 nM TTX. (*B*) Peak current-voltage (*I-V*) plot of whole-cell I_{Na} evoked with the test potentials of −60 to +60 mV with 10 mV increments. Solutions were the same as in *A* except for the *Choline* cell which was exposed to solution IV. *I-V* curves represent I_{Na} elicited in normal bath solution (open circles, 140 mM Na^+), with reduced $[Na^+]_o$ (filled circles, 70 mM Na^+ and 70 mM choline), and after the cell was treated with 100 mM TTX (open triangles, 140 mM Na^+).

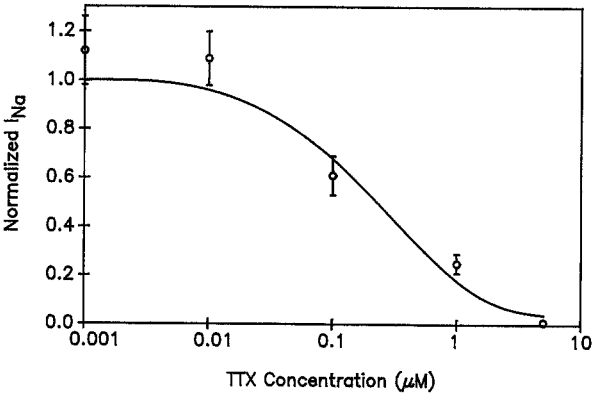

Fig. 5. The dose-response curve illustrating TTX inhibition of the voltage-dependent sodium currents in human small-cell lung cancer cells. The normalized peak I_{Na} is plotted against the concentration of TTX. Each data point is expressed as mean ± SEM of measurements from 18–68 H146 cells. The smooth curve is a fit to a one-to-one receptor binding model (Eq. 1), which yields a K_d of 215 nM.

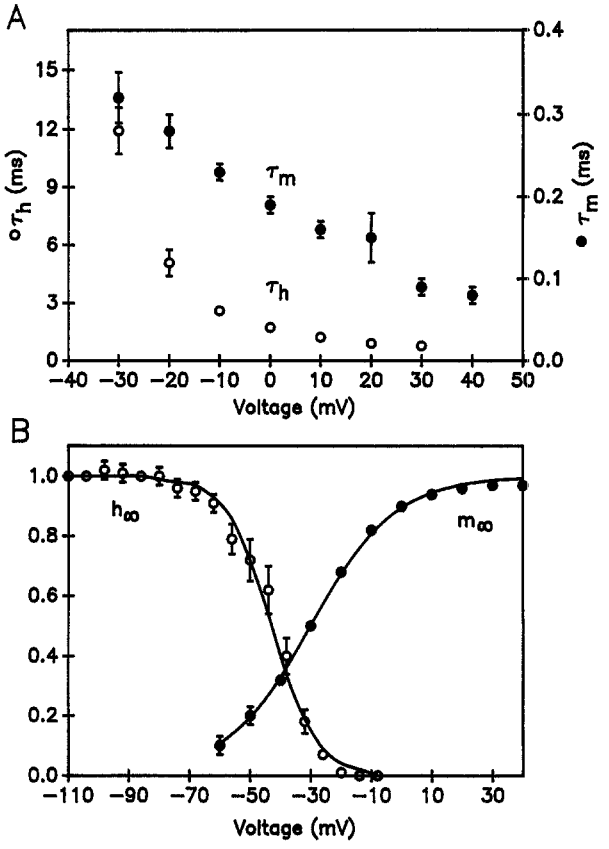

Fig. 6. Activation and inactivation kinetics of Na^+ current in SCLC cells. (*A*) Time constants of activation and inactivation of I_{Na}. The rising phase of I_{Na} was fit with the third power exponential function:

$$I(t) = A[1 - \exp(-t/\tau_m)]^p \quad (6)$$

where $I(t)$ is the current amplitude as a function of time, A is a constant, τ_m is the activation time constant and p is an integer. The decaying current was conformed to a single exponential function from which the inactivation time constant, τ_h, was determined. The filled circles represent τ_m (mean ± SEM) from 15 cells and the open circles describe τ_h from eighteen H146 cells. (*B*) The Hodgkin-Huxley steady-state activation, m_∞, and inactivation, h_∞, parameters of I_{Na}. m_∞ (filled circles) was determined by first applying 15 command pulses of 20 msec duration in 10 mV increments from −60 to +80 mV to the cell and then calculated from the equation:

$$m_\infty = (g_{Na}/g_{Na,max})^{1/3} = [1 + \exp(V_{1/2} - V)/a_m]^{-1} \quad (7)$$

where g_{Na} is the peak conductance at voltage V, $g_{Na,max}$ is the maximum peak conductance, $V_{1/2}$ is the half-activated potential, and a_m is the slope factor. Each data point represents mean ± SEM (n = 15 cells) and the continuous line is a plot of the above equation with the averaged $V_{1/2}$ and a_m. In characterizing the steady-state inactivation, h_∞ (open circles), prepulse potentials ranging from −110 to −8 mV in 6 mV increments for 50 msec, followed by a 40 msec test pulse to 0 mV, were applied to the cell. Normalized peak current was then plotted against prepulse potential and data were approximated by a Boltzmann function (Eq. 8) to obtain the half-inactivated potential $V_{1/2}$ and the slope factor, a_h:

$$h_\infty = I/I_{max} = [1 + \exp(V - V_{1/2})/a_h]^{-1} \quad (8)$$

$V_{1/2}$ and a_h were averaged from six cells and used to construct the continuous line.

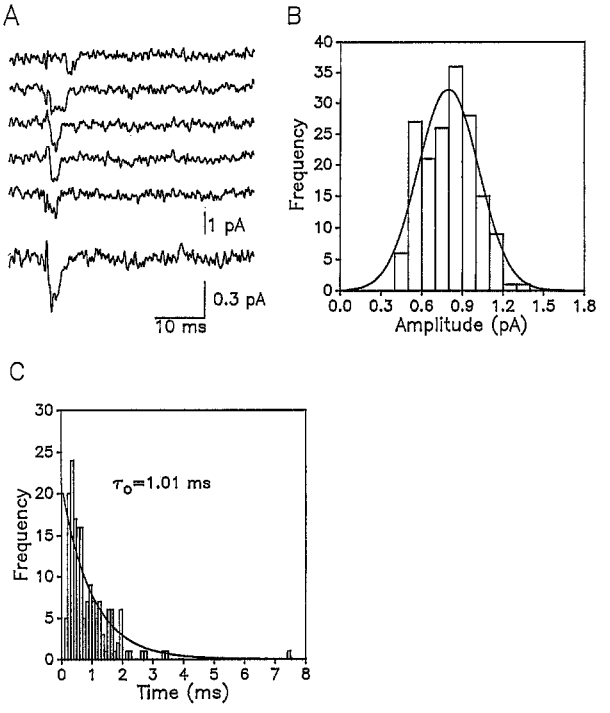

Fig. 7. Inside-out recording of an SCLC H146 single Na^+-channel current at −20 mV from a holding potential of −80 mV. (*A*) Five representative single channel traces are displayed. The bottom trace is the ensemble average of 126 traces. (*B*) The amplitude histogram shows a Gaussian distribution with a mean of 0.8 pA. (*C*) The open time histogram was fit with a single exponential. The time constant was found to be 1.0 msec. Internal and external solutions were V and II, respectively.

Inhibition of I_{Na} by LES Antibodies

Previously, it had been demonstrated that approximately 30% of LES patients produce antibodies that inhibit both I_{Na} and I_{Ca} in bovine adrenal chromaffin cells (Viglione et al., 1992). As SCLC cells are implicated in the disease process, we assessed whether LES serum or IgG could inhibit I_{Na} in the tumor cells. To test this hypothesis, we studied the effects of LES serum or IgG from three patients: Patient 1's IgG is known to inhibit both I_{Ca} and I_{Na} from our previous chromaffin cell study (Viglione et al., 1992), IgG from Patient 2 inhibited only I_{Ca} in bovine adrenal chromaffin cells, and serum from Patient 3 had not been previously tested. After 24 hr of exposure to serum from Patient 1 (1 mg/ml IgG), I_{Na} from H146 cells was significantly reduced from 53.8 ± 7.6 pA/pF ($n = 35$) to 31.5 ± 3.7 pA/pF ($n = 37$, $P < 0.05$), a decrement of 41% (Fig. 8*C*). The *I-V* curves and the corresponding current traces at +10 mV depolarization of a control and a LES serum-treated cell are shown in Fig. 8*A* and *B*, respectively. The reduction observed after 24 hr of incubation with the LES serum appeared to be maximal, as increasing the exposure time to 72 hr produced a reduction of 36% (control I_{Na}: 60.7 ± 6.6 pA/pF, $n = 22$, vs. LES I_{Na}: 38.4 ± 5.1 pA/pF, $n = 22$, $P < 0.05$). To determine which component(s) of the serum is bringing about the inhibition of the Na^+ channels, we repeated the previous experiments with IgG isolated from the serum of Patient 1. In contrast to the reduction observed after 24 hr with the serum, 1 mg/ml IgG did not significantly reduce I_{Na}. With 72 hr of incubation in the IgG, however, the currents declined from a control value of 59.1 ± 7.8 pA/pF ($n = 16$) to 41.3 ± 4.0 pA/pF ($n = 16$, $P < 0.05$) (Fig. 8*C*). Thus, it may be that the LES serum contains additional factors which speed the antibody-mediated inhibition of the Na^+ channels (for example, *see* Kim & Neher, 1988).

We had previously demonstrated that IgG from Patient 2 was not able to significantly inhibit I_{Na} in chromaffin cells (Viglione et al., 1992). Consistent with this observation, IgG from Patient 2 did not inhibit I_{Na} in SCLC cells; however, the antibodies were capable of reducing I_{Ca} (Viglione & Kim, 1993; Viglione, O'Shaughnessy & Kim, 1994). Serum from Patient 3, likewise, had been shown to be effective in reducing I_{Ca} in SCLC cells. However, after 48 hr of incubation in serum from this patient, a reduction in SCLC I_{Na} was not seen. Therefore, these results confirm and extend the previous conclusion (Viglione et al., 1992) that heterogeneity of antibodies exists among different LES patients, leading to the differential cross-reactivity of the pathogenic IgG with voltage-dependent Na^+ channels.

Discussion

Small-cell lung cancer was previously thought to originate from the Kulchitsky cells of the bronchial mucosa (Havemann et al., 1985), but recent reports suggest that SCLC is derived from the primitive endodermal cells which differentiate into neuroendocrine cells (Pietra, 1990). SCLC cells contain dense-core granules which may relate to the production and release of ectopic hormones such as adrenocorticotropic hormone, gastrin-releasing peptide and antidiuretic hormone. Recent patch clamp studies of human SCLC cells (Pancrazio et al., 1989) revealed the presence of voltage-dependent ion channels, including calcium channels that participate in Ca^{2+}-dependent exocytosis by these tumor cells (Kim, Pancrazio & Viglione, 1989).

Voltage-gated Na^+ channels are found in many excitable cells and play a primary role in the generation of action potentials. In this study of human small-cell lung cancer cells, we have investigated the ionic component which contributes to the spiking electrical behavior and examined the biophysical and pharmacological properties of the voltage-activated sodium channels. Additionally, we have examined whether Na^+ channels in these tumor cells are affected by antibodies from patients with LES.

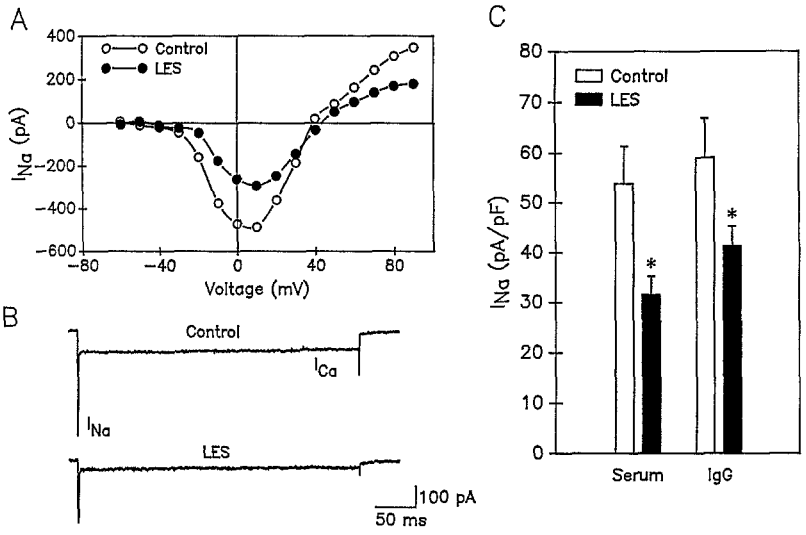

Fig. 8. Effect of LES serum and IgG on I_{Na} of SCLC cells. (*A*) *I-V* relationship of I_{Na} obtained from a control (open circles) and an LES serum (filled circles)-treated cell. Cells were incubated with control and LES serum for 24 hr at 1 mg/ml IgG concentration. (*B*) The corresponding current traces at +10 mV depolarization are plotted. (*C*) Reduction of I_{Na} by LES antibodies (1 mg/ml). Cells were incubated with control and LES serum for 24 hr and IgG isolated from the same serum for 72 hr. $^*P < 0.05$.

Role of Na^+ and Ca^{2+} Currents in the Spiking Electrical Behavior

Three observations from our study lead to the conclusion that Na^+ current in SCLC H146 tumor cells is primarily responsible for the generation of action potentials: (i) the all-or-nothing action potentials were blocked by 5 μM TTX in all cells examined, with no detectable change of transmembrane potentials; (ii) likewise, the spikes could not be evoked in a Na^+-free bath; and (iii) in contrast, full-size action potentials persisted in Ca^{2+}-free bath solution containing 1 mM $CoCl_2$. Data presented by Johansson et al. (1989) are in agreement with the observations presented in this study.

The results of our $MnCl_2$ experiments further support the conclusion that Na^+ channels are responsible for action potentials in these tumor cells. In their previous work on DMS 53 small-cell lung cancer cells, McCann et al. (1981) used $MnCl_2$ to block the putative Ca^{2+} spikes and interpreted their data as indicating that Ca^{2+} ions were the primary ions responsible for action potential generation. We ascertained that $MnCl_2$ also caused a significant reduction in I_{Na} in SCLC cells (Fig. 2*A*). Furthermore, in a Ca^{2+}-free external environment, we were able to reproduce the spike-inhibiting action of $MnCl_2$. Despite the absence of external Ca^{2+}, action potentials that appeared upon anodal break excitation were reversibly blocked by 4 mM $MnCl_2$. These results suggest that the diminution of the anodal break response in these experiments is the direct result of the blockade of Na^+ channels, rather than Ca^{2+} channels.

It could be argued that the heterogeneity of electrical characteristics governing the production of action potentials may exist among different SCLC cell lines such that the impulses in DMS 53 cells and H146 cells are initiated via characteristically different ionic conductance mechanisms. Although it is true that the relative expression of Na^+ and Ca^{2+} channels differ markedly from one SCLC cell line to the other (Pancrazio et al., 1989; Pancrazio et al., 1992), Ca^{2+} channel density in all cell lines tested so far appears to be relatively low. Of the six cell lines (H69, H82, H128, H146, H187, and H209) from which we have measured I_{Ca} (*unpublished observations*), H146 cells exhibit the largest I_{Ca}, and in a given cell, the amplitude of I_{Ca} (122.4 ± 6.2 pA, n = 131, as measured using 10 mM Ca^{2+} external solution) is consistently smaller than that of I_{Na} (for example, *see* Fig. 3*B*). These findings also support the notion that SCLC cells are unlikely to exhibit Ca^{2+}-spike electrogenesis. It should be noted, however, that we do not know what the resting potential of SCLC cells is in vivo. In our system, the resting potential is approximately −44 mV, a level sufficient to inactivate most of the Na^+ channels. Therefore, caution is warranted in predicting what the action potential behavior of these cells is in vivo.

TTX Sensitivity

TTX is a specific Na^+ channel blocker and is used as a probe for voltage-dependent Na^+ channels in various cell types. Based on the degree of TTX sensitivity, a number of studies have identified the existence of two populations of Na^+ channels in neurons (Ogata & Tatebayashi, 1992), cancer cells (Flamm, Birnberg & Kaczmarek, 1990; Weiss & Sidell, 1991), muscle cells and their precursors (Frelin et al., 1984; Weiss & Horn, 1986). The most distinguishing parameter for identifying the two types of Na^+ channels is the TTX affinity or K_d, derived from the dose-response relationship of TTX and channel inhibition. There is now general agreement that TTX-sensitive channels have a K_d in the low nanomolar level (<20 nM), whereas TTX-resistant types have a K_d in the high nanomolar and low micromolar range (100 nM to 10

μM). The wide disparity in the K_ds of these two channel subtypes is reflected in the shape of the TTX dose-response curve; a biphasic curve signifies the presence of more than one type of Na^+ channel, while a sigmoidal curve indicates a single population of Na^+ channels.

We found that the overall shape of the TTX dose-response curve obtained from human SCLC cells was sigmoidal, lacking a distinctive biphasic characteristic. The curve was better fit with a one-site model (Eq. 1) than the two-site, noncooperative model (Eq. 2). This finding is interpreted as indicating that SCLC cells express a single population of Na^+ channels, which are only weakly sensitive to TTX (K_d = 215 nM). The activation and inactivation kinetics found in SCLC H146 cells are similar to those found in the "TTX-resistant" channels of rat dorsal root ganglion cells (Ogata & Tatebayashi, 1992).

Whole-Cell I_{Na} in SCLC Cells

There are vast discrepancies in the amplitude of the Na^+ currents among SCLC NCI cell lines. Cells from NCI-H82 and H209 cell lines have considerably smaller I_{Na} than that measured in H146 cells (*unpublished observation*). Similar findings were reported by Pancrazio et al. (1989) who studied NCI-H69 and NCI-H128 cell lines. I_{Na} was observed in only 30% of H69 cells, and in H128 cells, I_{Na} was 3.2 ± 0.4 pA/pF, a more than 20-fold difference from the Na^+ currents recorded in H146 cells (73.19 ± 9.8 pA/pF). These differences reflect a heterogeneous expression of voltage-dependent Na^+ channels in small-cell tumor cells.

A commonly observed biophysical characteristic of I_{Na} is that it activates rapidly and inactivates in a single or double exponential time course depending on the cell type. The time constant of inactivation decreases with increasing depolarization. In H146 lung cancer cells, we have likewise demonstrated these properties typical of Na^+ channels, similar to other cancer cell lines (Johansson et al., 1989; Pancrazio et al., 1989), endocrine cells (Fenwick et al., 1982; Plant, 1988) and excitable cells (Carbone & Lux, 1986; Barres et al., 1989).

The single Na^+ channel conductance ranges from 8.7 pS in rat brain cells (Kirsch & Brown, 1989) to 27.8 pS in cardiac cells from neonatal rats (Cachelin et al., 1983). Most cell types have Na^+ conductances between 10 to 20 pS regardless of the recording conditions (Carbone & Lux, 1986; Barres et al., 1989). The Na^+ channel conductance in H146 cells is 12.3 pS, well within the reported range of conductances for Na^+ channels. In conclusion, the voltage-gated Na^+ channels in human small-cell lung cancer cells possess electrophysiological characteristics which are very similar to those found in many excitable cell types.

Clinical Perspective

The autoantibodies directed against voltage-dependent Ca^{2+} channels have been identified as a key pathogenic factor underlying the Lambert-Eaton myasthenic syndrome. IgG from patients with LES is known to inhibit the function of Ca^{2+} channels in bovine adrenal chromaffin cells (Kim & Neher, 1988), rodent neuroblastoma cells (Peers et al., 1990) and human small-cell lung cancer cells (Viglione & Kim, 1993; Viglione et al., 1994). As the majority of LES patients manifest the concurrent development of SCLC, the role played by the tumor cells in the etiology has attracted particular attention. The immunological event in which the Ca^{2+} channels expressed by SCLC cells act as the putative stimulatory antigens in this disorder is supported by our recent observation that LES antibodies react with Ca^{2+} channels in SCLC cells and block their function (Viglione & Kim, 1993; Viglione et al., 1994). It is interesting to note that the observations with serum or IgG from Patients 1 and 2 on SCLC cells are similar to our observations with chromaffin cells (Kim & Neher, 1988; Viglione et al., 1992). Both patients' antibodies reduced I_{Ca} in both cell types, but only IgG from Patient 1 affected I_{Na} in chromaffin and SCLC cells. Since Ca^{2+} and Na^+ channels have rather conserved structural similarity (Catterall, 1988), one may speculate that LES IgG recognizes the same antigenic site shared by both Na^+ and Ca^{2+} channels. Thus, a single species of antibodies could mediate the inhibition of both I_{Ca} and I_{Na}. The serum/IgG from each of the patients used in this study has been previously shown to inhibit I_{Ca} in SCLC cells. As demonstrated here, despite the inhibitory action of I_{Ca}, two of the patients' antibodies did not reduce I_{Na}. Therefore, another possibility is that the autoantibodies mediating the effects on Na^+ channels are a population distinct from those affecting Ca^{2+} channels. In this case, Na^+ channels, such as those characterized in the present work, are clearly the antigenic candidate.

This study was supported by National Institutes of Health grant NS18607 and a research grant from the Muscular Dystrophy Association. Dr. Y.I. Kim is the recipient of a Javits Neuroscience Investigator Award from the National Institute of Neurological Disorder and Stroke.

References

Anderson, N.E., Cunningham, J.M., Posner, J.B. 1987. Autoimmune pathogenesis of paraneoplastic neurological syndromes. *Crit. Rev. Neurobiol.* **3**:245–299

Antoni, H., Böcker, D., Eickhorn, R. 1988. Sodium current kinetics in intact rat papillary muscle: measurements with the loose-patch-clamp technique. *J. Physiol.* **406**:199–213

Århem, P. 1980. Effects of some heavy metal ions on the ionic currents of myelinated fibres from *Xenopus laevis*. *J. Physiol.* **306**:219–231

Barres, B.A., Chun, L.L.Y., Corey, D.P. 1989. Glial and neuronal

forms of the voltage-dependent sodium channel: characteristics and cell-type distribution. *Neuron* **2:**1375–1388

Cachelin, A.B., De Peyer, J.E., Kokubun, S., Reuter, H. 1983. Sodium channels in cultured cardiac cells. *J. Physiol.* **340:**389–401

Carbone, E., Lux, H.D. 1986. Sodium channels in cultured chick dorsal root ganglion neurons. *Eur. Biophys. J.* **13:**259–271

Carney, D.N. 1992. Biology of small-cell lung cancer. *Lancet* **339:**843–846

Catterall, W.A. 1988. Structure and function of voltage-sensitive ion channels. *Science* **242:**50–60

Decoursey, T.E., Chandy, K.G., Gupta, S., Cahalan, M.D. 1984. Voltage-gated K^+ channels in human T-lymphocytes: a role in mitogenesis? *Nature* **307:**466–468

Elmqvist, D., Lambert, E.H. 1968. Detailed analysis of neuromuscular transmission in a patient with the myasthenic syndrome sometimes associated with bronchogenic carcinoma. *Mayo Clin. Proc.* **43:**689–713

Fenwick, E.M., Marty, A., Neher, E. 1982. Sodium and calcium channels in bovine chromaffin cells. *J. Physiol.* **331:**599–635

Flamm, R.E., Birnberg, N.C., Kazcmarek, L.K. 1990. Transfection of activated rats into an excitable cell line (AtT-20) alters tetrodotoxin sensitivity of voltage-dependent sodium current. *Pfluegers Arch.* **416:**120–125

Frelin, C., Vijverberg, H.P.M., Romey, G., Vigne, P., Lazdunski, M. 1984. Different functional states of tetrodotoxin sensitive and tetrodotoxin resistant Na^+ channels occur during the in vitro development of rat skeletal muscle. *Pfluegers Arch.* **402:**121–128

Hamill, O.P., Marty, A., Neher, E., Sakmann, B., Sigworth, F.J. 1981. Improved patch-clamp techniques for high-resolution current recording from cells and cell-free membrane patches. *Pfluegers Arch.* **391:**85–100

Havemann, K., Luster, W., Gropp, C., Holle, R. 1985. Peptide hormone production associated with small cell lung cancer. *In:* Small Cell Lung Cancer. C. Seeber editor. pp. 65–76. Springer, Heidelberg

Hodgkin, A.L., Huxley, A.F. 1952. A quantitative description of membrane current and its application to conduction and excitation in nerve. *J. Physiol.* **117:**500–544

Isenberg, G., Klöckner, U. 1982. Isolated bovine ventricular myocytes characterization of the action potential. *Pfluegers Arch.* **395:**19–29

Johansson, S., Rydqvist, B., Swerup, C., Heilbronn, E., &rhem, P. 1989. Action potentials of cultured human oat cells: whole-cell measurements with the patch-clamp technique. *Acta Physiol. Scand.* **135:**573–578

Kim, Y.I., Neher, E. 1988. IgG from patients with Lambert-Eaton syndrome blocks voltage-dependent calcium channels. *Science* **239:**405–408

Kim, Y.I., Pancrazio, J.J., Viglione, M.P. 1989. Calcium-dependent exocytosis and the type of calcium channels in a small-cell lung cancer cell line. *Soc. Neurosci. Abstr.* **15:**824

Kirsch, G.E., Brown, A.M. 1989. Kinetic properties of single sodium channels in rat heart and rat brain. *J. Gen. Physiol.* **93:**85–99

Lee, Y.S., Weber, M., Wurster, R.D. 1992. Roles of Ca^{2+} and K^+ in nervous system tumor cell growth. *Soc. Neurosci. Abstr.* **18:**1360

McCann, F.V., Pettengill, O.S., Cole, J.J., Russell, J.A.G., Sorenson, G.D. 1981. Calcium spike electrogenesis and other electrical activity in continuously cultured small cell carcinoma of the lung. *Science* **212:**1155–1157

Ogata, N., Tatebayashi, H. 1992. Ontogenic development of the TTX-sensitive and TTX-insensitive Na^+ channels in neurons of the rat dorsal root ganglia. *Dev. Brain Res.* **65:**93–100

Pancrazio, J.J., Oie, H.K., Kim, Y.I. 1992. Voltage-sensitive calcium channels in a human small-cell lung cancer cell line. *Acta Physiol. Scand.* **144:**463–468

Pancrazio, J.J., Viglione, M.P., Kleiman, R.J., Kim, Y.I. 1991. Verapamil-induced blockade of voltage-activated K^+ current in small-cell lung cancer cells. *J. Pharmacol. Exp. Ther.* **257:**184–191

Pancrazio, J.J., Viglione, M.P., Tabbara, I.A., Kim, Y.I. 1989. Voltage-dependent ion channels in small-cell lung cancer cells. *Cancer Res.* **49:**5901–5906

Peers, C., Lang, B., Newsom-Davis, J., Wray, D.W. 1990. Selective action of myasthenic syndrome antibodies on calcium channels in a rodent neuroblastoma x glioma cell line. *J. Physiol.* **421:**293–308

Pietra, G.G. 1990. The pathology of carcinoma of the lung. *Semin. Roentgen.* **25:**25–33

Plant, T.D. 1988. Na^+ currents in cultured mouse pancreatic B-cells. *Pfluegers Arch.* **411:**429–435

Roberts, A., Perera, S., Lang, B., Vincent, A., Newsom-Davis, J. 1985. Paraneoplastic myasthenic syndrome IgG inhibits $^{45}Ca^{2+}$ influx in a human cell carcinoma line. *Nature* **317:**737–739

Tischler, A.S., Dichter, M.A., Biales, B. 1977. Electrical excitability of oat cell carcinoma. *J. Pathol.* **122:**153–156

Viglione, M.P., Creutz, C.E., Kim, Y.I. 1992. Lambert-Eaton syndrome: antigen-antibody interaction and calcium current inhibition in chromaffin cells. *Muscle Nerve* **15:**1325–1333

Viglione, M.P., Kim, Y.I. 1993. Lambert-Eaton syndrome serum inhibits P-type calcium channels in small-cell lung cancer cells. *Soc. Neurosci. Abstr.* **19:**703

Viglione, M.P., O'Shaughnessy, T.J., Kim, Y.I. 1994. P-type calcium channels in human small-cell lung cancer cells: down regulation by Lambert-Eaton syndrome antibodies. *Biophys. J.* **66:**A422 (*Abstr.*)

Vincent, A., Lang, B., Newsom-Davis, J. 1989. Autoimmunity to the voltage-gated calcium channel underlies the Lambert-Eaton myasthenic syndrome, a paraneoplastic disorder. *TINS* **12:**496–502

Weiss, R.E., Horn, R. 1986. Single-channel studies of TTX-sensitive and TTX-resistant sodium channels in developing rat muscle reveal different open channel properties. *Ann. NY Acad. Sci.* **479:**152–161

Weiss, R.E., Sidell, N. 1991. Sodium currents during differentiation in a human neuroblastoma cell line. *J. Gen. Physiol.* **97:**521–539